Dirac fermions in armchair graphene nanoribbons trapped by electric quantum dots

Vít Jakubský [1], Şengul Kuru [2], and Javier Negro [3]
[1]*Nuclear Physics Institute, Czech Academy of Science, 250 68 Řež, Czech Republic*
[2]*Department of Physics, Faculty of Science, Ankara University, 06100 Ankara, Turkey*
[3]*Departamento de Física Teórica, Atómica y Óptica, Universidad de Valladolid, 47011 Valladolid, Spain*

(Received 2 December 2021; revised 26 February 2022; accepted 4 March 2022; published 4 April 2022)

We study the confinement of Dirac fermions in armchair graphene nanoribbons by means of electrostatic quantum dots. We provide an analytically feasible model where some bound states can be found explicitly. We show that the energies of these bound states belong either to the gap of valence and conducting bands or they represent bound states in the continuum whose energies are embedded in the continuous spectrum. The solutions satisfying armchair boundary conditions are found in an elegant manner with the use of specific projection operators.

DOI: 10.1103/PhysRevB.105.165404

I. INTRODUCTION

Electrostatic barriers are transparent for massless Dirac fermions with normal incidence due to Klein tunneling [1]. Therefore, electrostatic confinement of massless Dirac fermions in graphene is difficult. In the oblique direction, the nonzero tangent momentum gives rise to an effective mass term and reflection on the barrier is possible.

It was predicted theoretically and observed experimentally that despite the Klein tunneling, there are resonant modes called quasibound states that are trapped for very long times by the electrostatic field [2–12], see also Ref. [13]. They arise due to constructive interference of the reflected waves within the quantum dot, in analogy to whispering-gallery modes in acoustic cavities [14]. The quasibound states, characterized by outgoing boundary conditions and nonvanishing yet small imaginary parts of the energy, were analyzed theoretically in circular graphene quantum dots [2–7], as well as in the systems with rectangular geometry in plane [8], or in carbon (arm-chair) nanoribbons [9–12]. In the later work, they were suggested in the role of possible spin qubit system.

Electrostatic quantum dots can even confine bound states with exponentially decaying wave functions outside the potential well. Their existence was revealed in systems with translational symmetry [15–19]. Confinement of zero-energy Dirac fermions by electrostatic quantum dots with rotational symmetry was showed analytically in Refs. [20–22]. Bound states in circular quantum dots with nonvanishing energy were discussed in Ref. [4]. Electronic transport of Dirac fermions in armchair nanoribbons in the presence of a rectangular electrostatic barrier dependent on a single coordinate was studied in Refs. [9,12]. A similar setting with an additional inhomogeneity of Fermi velocity was taken into account in Ref. [23]. In Ref. [24], the confinement of Dirac fermions of nonzero energy by a periodic chain of electrostatic scatterers was demonstrated.

Theoretical studies of the quasibound states as well as bound states confined by the electrostatic field have been accompanied by experimental results. Electrostatic quantum dots with circular geometry can be created by the tips of scanning tunneling microscope (STM). Existence of the quasibound states created by the STM or by substrate manipulations was reported in Refs. [14,25–27]. In Ref. [28], a modified STM tip was used for the creation of circular quantum dots with tunable size from nanometers to micrometers. The bound states were observed for deep, small potential wells of nanometer scale, whereas whispering-gallery modes were reported for the quantum dots of larger scale. The existence of bound states was also confirmed experimentally in Ref. [29].

Bound states in a quantum system can correspond either to discrete energies or to energies embedded in the continuum. In the latter case, they are called BICs (bound states in the continuum). Existence of BICs in physical systems was anticipated back in 1929 by von Neumann and Wigner [30]. Despite their coexistence with scattering states of infinitely close energies, they do not couple to them. They can be understood as resonances with infinitely long decay rates. Since, BICs have been studied in a wide range of physical scenarios; see Ref. [31] for extensive review. In the context of graphene, they have an important role in the design of graphene-based electronic and optical devices with tunable transport [32,33] and optical properties [34,35].

In the current paper, we present an analytically tractable model of quantum dots in an arm-chair graphene nanoribbon (AGNR) that confines bound states of nonzero energy. Although the model lacks both translational and rotational symmetry, we show that there can be confined bound states with nonzero energies that are either in the spectral gap or belong to the continuum spectral band and correspond to BICs. The corresponding wave functions are given by analytical closed expressions. To facilitate their calculation, we propose the method of projection operators based on symmetries of

the two-valley Dirac equation. The projectors map the generic solutions of the stationary equation into those that comply with the boundary conditions. This approach is rather general and can be applied to a wider class of systems than those presented in this paper.

The stationary equation of free Dirac massless fermions in graphene can be written in the following form [36]:

$$H_0\Psi = (\tau_0 \otimes \sigma_1 p_x + \tau_0 \otimes \sigma_2 p_y)\Psi = E\Psi, \tag{1}$$

where both τ_j and σ_j, $j = 1, 2, 3$, are Pauli matrices, and τ_0 and σ_0 are 2×2 identity matrices. The matrices τ_j act on the valley degree of freedom associated to the Dirac points $\mathbf{K}$ and $\mathbf{K}'$ of graphene. The matrices σ_j act on the sublattice degree of freedom related to presence of two triangular sublattices $\mathbf{A}$ and $\mathbf{B}$. For convenience, we identify the components $\psi(')_X$ of Ψ in Eq. (1) with the sublattices and valleys as follows, see Ref. [36]:

$$\Psi := (\psi_A, \psi_B, \psi'_B, -\psi'_A). \tag{2}$$

For instance, $\psi_A(')(\mathbf{r})$ describes Dirac fermions localized at the lattice A with momentum near the Dirac point $\mathbf{K}(')$. The interpretation of the other components goes in the same manner.

In graphene nanoribbons, the solutions of Eq. (1) are subject to the boundary conditions that characterize the edges of the graphene strip. The boundary conditions were discussed in a number of works [36–39].We adopt here the notation of Ref. [36] in which the stationary equation of the free Dirac fermion coincides with Eq. (1).[1]

The boundary condition at boundary Γ can be specified in terms of a unitary matrix M as follows:

$$\Psi|_{\vec{x}\in\Gamma} = M\Psi|_{\vec{x}\in\Gamma}, \quad M^\dagger = M, \quad M^2 = 1. \tag{3}$$

To avoid the leaks of probability current through the boundary, the matrix has to satisfy

$$\{M, \mathbf{n_B}.\mathbf{J}\} = 0, \tag{4}$$

where $\mathbf{n_B} = \{n_1, n_2, 0\}$ is the normal vector to the boundary and $\mathbf{J} = (\tau_0 \otimes \sigma_1, \tau_0 \otimes \sigma_2, 0)$ is the current density operator. Together with the requirement of the time-reversal symmetry [36], the matrix M acquires the following general form:

$$M = \boldsymbol{\nu} \cdot \boldsymbol{\tau} \otimes \mathbf{n_1} \cdot \boldsymbol{\sigma}, \tag{5}$$

where $\boldsymbol{\tau} = \{\tau_1, \tau_2, \tau_3\}$, $\boldsymbol{\sigma} = \{\sigma_1, \sigma_2, \sigma_3\}$; $\mathbf{n_1}$ is a unit vector perpendicular to $\mathbf{n_B}$ and $\boldsymbol{\nu}$ is an arbitrary three-dimensional unit vector. Let us mention two specific families of the boundary conditions. In the first case, the boundary condition does not mix the valleys:

$$M = \tau_3 \otimes \sigma_3 e^{i\nu\sigma_1}, \quad \nu \in (-\pi, \pi]. \tag{6}$$

When $\nu = 0$, M represents a zigzag boundary condition. For $\nu = \pm\pi/2$, it describes infinite-mass boundary condition. The other values of ν can be attributed to the presence of staggered potential at the boundary, see Ref. [36]. The second family corresponds to an armchairlike boundary:

$$M = \tau_1 e^{i\alpha\tau_3} \otimes \sigma_1 e^{i\mu\sigma_3}, \quad \alpha, \mu \in (-\pi, \pi]. \tag{7}$$

Here μ depends on the explicit form of $\mathbf{n_B}$ whereas parameter α can be attributed to width L of the nanoribbon.

It is worth mentioning that the armchair boundary conditions are less universal than zigzag graphene nanoribbons boundary conditions with $M = \tau_3 \otimes \sigma_3$, which apply to a wider range of lattice terminations [36]. Nevertheless, AGNRs attract attention due to the energy gap that opens between positive and negative energies, which is desirable in electronic devices. Additionally, it proved to be possible to fabricate highly precise AGNR in the experiments [40].

We will present a model where Dirac fermions in AGNR are confined by a strongly localized electrostatic field. But first, it is convenient to briefly review the spectral properties of free Dirac fermions in an armchair nanoribbon, since it will be quite helpful for the following analysis of the electric quantum dots.

II. FREE PARTICLES IN AGNR

Let us consider an armchair nanoribbon of width L which is oriented along the y axis, i.e., $x \in [0, L]$ and $y \in \mathbb{R}$. The normal vector $\mathbf{n_B}$ perpendicular to the boundary and pointing outward is $\mathbf{n_B} = (-1, 0, 0)$ for $x = 0$ and $\mathbf{n_B} = (1, 0, 0)$ for $x = L$. Therefore, we can see from Eqs. (4) and (7) that the matrices M_1 and M_2 fixing the boundary conditions at $x = 0$ and $x = L$, respectively, can be defined without lack of generality as[2]

$$M_1 = \tau_1 \otimes \sigma_2, \quad M_2 = \tau_1 e^{i\alpha\tau_3} \otimes \sigma_2, \quad \alpha \in (-\pi, \pi]. \tag{8}$$

For the armchair nanoribbon without any additional interaction at the boundary, the parameter α can be associated with the width L of the nanoribbon. Its origin can be traced back to the tight-binding model. Indeed, the solutions of the Dirac Eq. (1) correspond to the slowly varying amplitudes $\psi_A(')$, $\psi_B(')$ of the total wave functions defined on sublattices A and B, see Refs. [37,41]:

$$\Psi_A = e^{iKx}\psi_A - ie^{iK'x}\psi'_A, \quad \Psi_B = e^{iKx}\psi_B - ie^{iK'x}\psi'_B. \tag{9}$$

Remember that the Dirac points are $\mathbf{K} = (K, 0) = (\frac{2\pi}{3a_0}, 0)$ and $\mathbf{K}' = (K', 0) = -\mathbf{K}$, where a_0 is the constant of the lattice. The armchair boundaries are formed by the atoms from both sublattices A and B. The corresponding total wave functions should be vanishing there:

$$(\psi_X(x, y)e^{iKx} - i\psi'_X(x, y)e^{iK'x})|_{\substack{x=0\\x=L}} = 0, \quad X = A, B, \ \forall y. \tag{10}$$

Comparing these relations with Eqs. (8), we get $\alpha = 2KL = \frac{4\pi}{3a_0}L$. Therefore, for nanoribbons with no additional edge

[1] Hamiltonian used by Brey *et al.* in Ref. [37] reads $H_B = \tau_3 \otimes \sigma_1 p_x + \tau_0 \otimes \sigma_2 p_y$ whereas the Hamiltonian used by Akhmerov *et al.* in Ref. [36] is $H_A = \tau_0 \otimes (\sigma_1 p_1 + \sigma_2 p_2)$. The mapping between the two operators is mediated by the operator $U = \begin{pmatrix} \sigma_0 & 0 \\ 0 & -\sigma_2 \end{pmatrix}$. There holds $H_B = U H_A U^{-1}$.

[2] Indeed, if the wave function Ψ satisfies $(1 - M_1)\Psi(0, y) = 0$ and $(1 - M_2)\Psi(L, y) = 0$, then the wave function $\tilde{\Psi} = e^{i\beta\tau_3}\Psi$ satisfies $(1 - \tilde{M}_1)\tilde{\Psi}(0, y) = 0$ and $(1 - \tilde{M}_2)\tilde{\Psi}(L, y) = 0$, where $\tilde{M}_1 = \tau_1 e^{-2i\beta\tau_3} \otimes \sigma_2$ and $\tilde{M}_2 = \tau_1 e^{i(\alpha-2\beta)\tau_3} \otimes \sigma_2$.

interactions, we get effectively $\alpha = 0$ for $L = 3Ma_0$ and $\alpha = \pm 2\pi/3$ for $L = (3M \pm 1)a_0$, where M is an integer, see Refs. [37,41]. Other values of α can reflect the presence of an additional interaction or altered crystal structure at the boundary [42].

The admissible solutions of the stationary Eq. (1) have to satisfy

$$H_0\Phi = E\Phi, \quad \Phi(0, y) = M_1\Phi(0, y),$$
$$\Phi(L, y) = M_2\Phi(L, y). \tag{11}$$

The boundary conditions Eqs. (10) have been replaced by matrix equations which allow for an easier algebraic manipulation, as will be shown in the following. This matrix form will play a fundamental role in our approach. We can find the wave functions $\Phi(x, y)$ in the following manner: the Hamiltonian H_0 commutes with the operator P_0M_1, $[H_0, P_0M_1] = 0$, where P_0 is reflection along the axis $y = 0$, i.e., $P_0 f(x, y) = f(-x, y)$. We can utilize this fact and define the wave function

$$\Phi(x, y) = (\mathbf{1} + P_0M_1)F(x, y), \tag{12}$$

where $F = F(x, y)$ is a generic solution of $(H_0 - E)F(x, y) = 0$ and $\mathbf{1} = \tau_0 \otimes \sigma_0$. By construction, Φ solves the same equation and additionally it satisfies the boundary condition at $x = 0$. Indeed, we have

$$\Phi(0, y) = (\mathbf{1} + P_0M_1)F(x, y)|_{x=0} = (\mathbf{1} + M_1)F(0, y)$$
$$= M_1(\mathbf{1} + M_1)F(0, y) = M_1\Phi(0, y), \tag{13}$$

where we used the fact that $M_1^2 = \mathbf{1}$. Hence, the operator $\mathbf{1} + P_0M_1$ works as a projector to the space of functions where the boundary condition at $x = 0$ is satisfied.[3] If we substitute the explicit form of Φ into the boundary condition at $x = L$, $(\mathbf{1} - M_2)\Phi(L, y) = 0$, and use $M_2^2 = \mathbf{1}$, we get the following equation:

$$(\mathbf{1} - M_2)(F(L, y) - M_2M_1F(-L, y)) = 0. \tag{14}$$

Therefore, when $F(x, y)$ satisfies

$$F(L, y) = M_2M_1F(-L, y) = e^{i\tau_3\alpha} \otimes \sigma_0 F(-L, y), \tag{15}$$

then $\Phi(x, y)$ defined by Eq. (12) fulfills the boundary conditions both at $x = 0$ and $x = L$.

Relation Eq. (15) requires the components of $F(x, y)$ to be quasiperiodic. It is rather straightforward to find the bispinors $F(x, y)$ such that Eq. (14) is satisfied. They are

$$F_{1,n}(x, y) = e^{ik_y y + i(\frac{n\pi}{L} + \frac{\alpha}{2L})x}\left(\frac{\frac{n\pi}{L} + \frac{\alpha}{2L} - ik_y}{\sqrt{\left(\frac{n\pi}{L} + \frac{\alpha}{2L}\right)^2 + k_y^2}}, 1, 0, 0\right),$$
$$F_{2,n} = \tau_1 \otimes \sigma_0 F_{1,n}|_{\substack{\alpha\to-\alpha \\ n\to-n}}, \quad n \in \mathbb{Z}, \tag{16}$$

where $(H_0 - E_n)F_{1(2),n} = 0$ and $E_n = \sqrt{(\frac{n\pi}{L} + \frac{\alpha}{2L})^2 + k_y^2}$. The corresponding bispinors that comply with the boundary conditions are

$$\Phi_{1,n} = (\mathbf{1} + P_0M_1)F_{1,n}, \quad \Phi_{2,n} = (\mathbf{1} + P_0M_1)F_{2,n}, \tag{17}$$

such that $(H_0 - E_n)\Phi_{j,n} = 0$, $j = 1, 2$.

The spectrum of a generic self-adjoint operator consists of two disjoint sets: the essential spectrum σ_{ess} and the discrete spectrum σ_d. In the case of the free-particle Hamiltonian H_0 with the domain specified by the boundary conditions Eqs. (8), there are no discrete eigenvalues. Its spectrum is formed just by the essential spectrum. The gap between positive and negative energies depends on the value of the parameter α:

$$\sigma(H_0) = \sigma_{\text{ess}}(H_0) = (-\infty, -E_0] \cup [E_0, \infty), \quad E_0 = \frac{|\alpha|}{2L}. \tag{18}$$

When $\alpha = 0$, i.e., $M_2 = M_1$ there is no gap in the spectrum so the nanoribbon is metallic. When $\alpha = \pi$, i.e., $M_2 = -M_1$, the spectral gap is maximal.

It is worth noticing that the construction of eigenstates via the projector Eq. (12) is rather general and can be applied to a large class of energy operators, see Appendix. Formula Eq. (15) suggests that it can be particularly useful for periodic systems where the wave functions are quasiperiodic due to the Bloch theorem. We will apply this construction in the next section.

III. ELECTROSTATIC QUANTUM DOTS IN AGNR

Now, let us analyze the possible confinement of Dirac fermions on armchair nanoribbons in the presence of electrostatic quantum dots described by the following stationary equation:

$$H\Psi = (H_0 + V(x, y))\Psi = E\Psi, \tag{19}$$

where H_0 is the free Hamiltonian given in Eq. (1) and the potential term has the following explicit form:

$$V(x, y) = -\sigma_0 \otimes \sigma_0 \frac{4m\omega^2 \sin^2 \kappa x}{m^2 + \omega^2 \cos 2\kappa x + \kappa^2 \cosh 2\omega y},$$
$$\kappa = \sqrt{m^2 + \omega^2}. \tag{20}$$

The parameters m and ω can acquire arbitrary nonvanishing real values. The sign of $V(x, y)$ corresponds to $-\text{sign}\, m$. Equation (19) was derived in Ref. [24] with the use of time-dependent supersymmetric transformation. In that work, analytical solutions for planar Dirac fermions of a specific, fixed energy $E = m$ were provided. We have no explicit knowledge of solutions for other energy values. Notice that the chiral symmetry of H_0 is broken in H by the presence of $V(x, y)$. Therefore, the spectrum of H is not necessarily symmetric with respect to zero. From now on, we fix $m > 0$ without loss of generality. This choice makes the electrostatic field $V(x, y)$ nonpositive. The results for $m < 0$ can be obtained in the same vain.

The term Eqs. (20) corresponds to an electrostatic potential which is periodic in x and decreases exponentially in y,

$$V(x, y) = V(x + T, y), \quad T = \frac{\pi}{\kappa},$$
$$V(x, y) \to 0, \text{ for } |y| \to \infty. \tag{21}$$

[3] At the boundary $x = 0$, the space of solutions of $(H_0 - E)F(x, y)|_{x=0} = 0$ is four-dimensional. The projector in Eq. (12) reduces into $\mathbf{1} + M_1$ at the boundary and projects the space of solutions into a two-dimensional subspace.

As the potential term is exponentially vanishing in y, its presence does not alter the essential spectrum of Dirac fermions in the nanoribbons—it does not alter the spectral gap. Therefore, there holds

$$\sigma_{\rm ess}(H) = \sigma_{\rm ess}(H_0), \tag{22}$$

see Lemma 3.4 in Ref. [43]. Nevertheless, there can emerge bound states due to the interaction with energies either in the gap or within the essential spectrum. Let us notice that exponentially vanishing electrostatic quantum dot was considered as a reasonable approximation of the experimental setting in Ref. [44].

The Hamiltonian Eq. (19) commutes both with P_0M_1 and P_0M_2:

$$[H, P_0M_1] = [H, P_0M_2] = 0, \tag{23}$$

where M_1 and M_2 are given in Eqs. (8).

Equation (19) has four solutions for $E = m$ that are strongly localized by the electrostatic field. The first one, v_1, has the following expression:

$$v_1(x,y) = \frac{1}{D(x,y)} \begin{pmatrix} -i\cosh(\omega y)[\kappa\cos(\kappa x) + m\sin(\kappa x)] + \omega\sin(\kappa x)\sinh(\omega y) \\ \cosh(\omega y)[-\kappa\cos(\kappa x) + m\sin(\kappa x)] + i\omega\sin(\kappa x)\sinh(\omega y) \\ 0 \\ 0 \end{pmatrix}, \tag{24}$$

where we abbreviated the denominator by the nonvanishing function $D(x,y) = m^2 + \omega^2\cos(2\kappa x) + \kappa^2\cosh(2\omega y)$. The other solutions, v_2, v_3, and v_4, are obtained from v_1 by

$$v_2(x,y) = \sigma_0 \otimes \sigma_3 v_1(-x,-y), \quad v_3 = \sigma_1 \otimes \sigma_0 v_1, \quad v_4 = \sigma_1 \otimes \sigma_0 v_2. \tag{25}$$

All of them have the same eigenvalue m:

$$Hv_a(x,y) = m\,v_a(x,y), \quad a = 1,2,3,4. \tag{26}$$

These wave functions are strongly localized along the y axis and are T antiperiodic in the x direction:

$$v_a(x,y) = -v_a(x+T,y). \tag{27}$$

Let us stress that the states $v_a(x,y)$ do not necessarily comply with the boundary conditions of the armchair nanoribbon. Nevertheless, we will consider two specific cases where localized states based on Eqs. (24) and (25) can be found.

A. AGNR with the maximal band gap

Let us focus on the specific case of the armchairlike boundary conditions Eqs. (8) where the spectral gap is maximal, i.e., $\alpha = \pi$ and $M_2 = -M_1$. We fine-tune the electrostatic field such that its period T_j can match the fixed width L of the nanoribbon in the following manner:

$$T_j = \frac{\pi}{\sqrt{m_j^2 + \omega_j^2}} = \frac{L}{j+1/2}, \quad j \in \{0,1,2,\dots\}. \tag{28}$$

Now we can follow the same steps as in case of the free particle model. We compose the wave functions Ψ_a as

$$\Psi_a = (\mathbf{1} + P_0M_1)v_a(x,y), \quad H\Psi_a = m_j\Psi_a, \quad a = 1,2,3,4, \tag{29}$$

which, by definition, comply with the boundary condition at $x = 0$. The eigenstates Eqs. (25) are T antiperiodic, $v_a(x,y) = -v_a(x+T,y)$, and satisfy

$$v_a(L,y) = M_1M_2v_a(-L,y) = -v_a(-L,y). \tag{30}$$

Then it is possible to show (see the Appendix) that Ψ_a satisfies the boundary conditions

$$(\mathbf{1} - M_1)\Psi_a(0,y) = 0, \quad (\mathbf{1} + M_1)\Psi_a(L,y) = 0, \quad a = 1,2,3,4. \tag{31}$$

Additionally, the bispinors Ψ_a are square integrable on $(x,y) \in [0,L] \times \mathbb{R}$ so they represent bound states confined by the electrostatic field. As their density of probability is essentially indistinguishable in the plots, we illustrate just one of them in Fig. 1 for different choices of parameters m, ω, and L.

The energy $E = m_j$ of the bound states Eq. (29) can be either in the energy gap or within the spectral band, i.e., immersed in the essential spectrum of H. In the latter case, we deal with the BICs. The position of the bound-state energy relative to the energy gap depends on the parameters $m \equiv m_j$ and $\omega \equiv \omega_j$ that define the electrostatic potential Eqs. (20). The condition Eqs. (28) does not fix the parameters m_j and ω_j uniquely. Indeed, with j being fixed, any of the configurations that satisfies $m_j^2 + \omega_j^2 = \frac{\pi^2(2j+1)^2}{4L^2}$ is admissible. These configurations differ by the energy m_j of the bound states Ψ_a:

$$m_j \in \left(0, \frac{\pi(2j+1)}{4L}\right). \tag{32}$$

The threshold of the essential spectrum $E_0 = \frac{\pi}{2L}$ stays within this interval for any $j \in \{1,2,\dots\}$ and, therefore, there exists m_j in Eq. (32) such that $m_j < E_0$ or such that $m_j > E_0$ for nonzero j. For $j = 0$, all the admissible values of m_0 lie below the threshold of the essential spectrum, $m_0 < E_0$; see Fig. 2 for illustration. We arrive at the following conclusions:

(1) If the period of the potential is $T_0 = 2L$, then the energy of the bound state is in the interval $0 < m_0 < E_0 = \frac{\pi}{2L}$ and, therefore, it belongs to the discrete spectrum $\sigma_d(H)$.

(2) If the period T_j of the potential is smaller, $j = 1,2,\dots$, then we have two options how to choose parameter m_j:

(i) $0 < m_j < E_0 = \frac{\pi}{2L}$,
(ii) $E_0 = \frac{\pi}{2L} < m_j < \frac{\pi(2j+1)}{2L}$.

If m_j satisfies (i), then the energy $E = m_j$ stays in the gap and belongs into $\sigma_d(H)$. When m_j satisfies (ii), the energy m_j

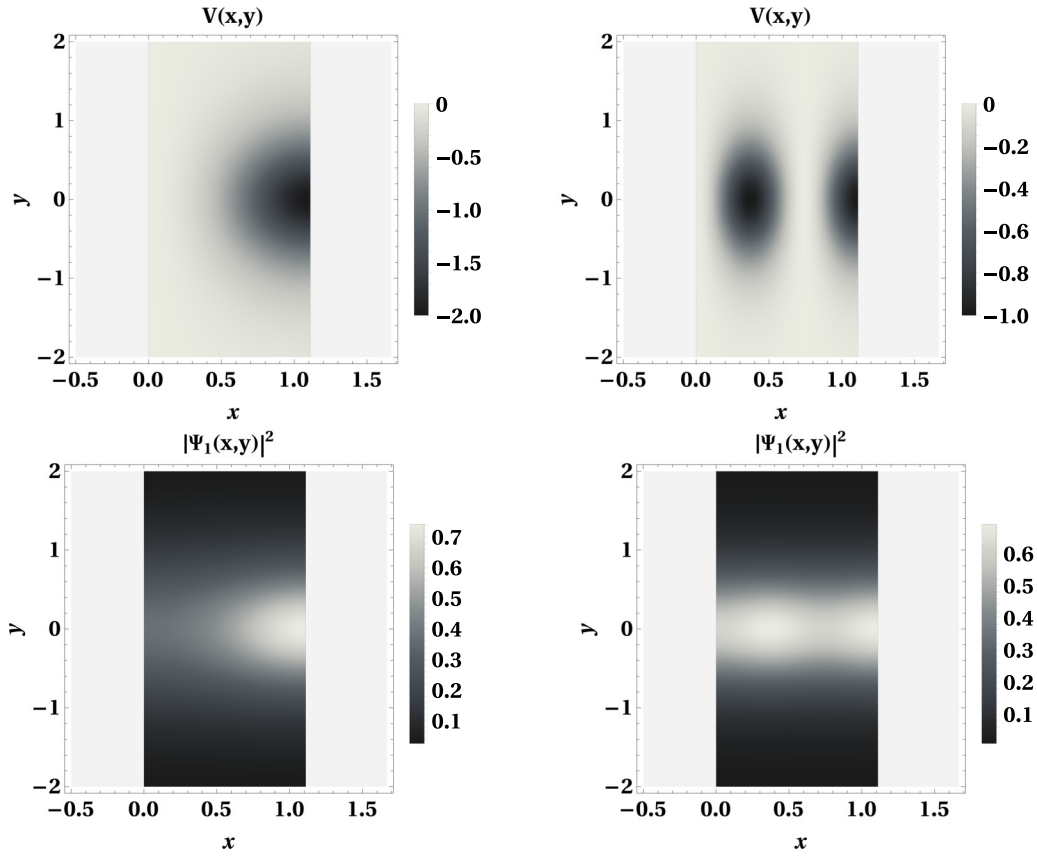

FIG. 1. Top: Electrostatic potential $V(x, y)$ in Eqs. (20). On the left, the potential has period $T_0 = 2L$ and $m_0 = 1$. The corresponding energy level $E \equiv m_0$ belongs to the discrete spectrum. On the right, there holds $T_1 = \frac{2L}{3}$ and $m_1 = 4$. In this case, the energy $E \equiv m_1$ of the bound states is embedded in the continuum. In both cases, $L = \frac{\pi}{2\sqrt{2}}$ and $\omega = \sqrt{\frac{\pi^2}{T^2} - m^2}$. Bottom: Density of probability of (normalized) Ψ_1 in Eqs. (29) for the boundary matrices $M_2 = -M_1$ and for the aforementioned values of parameters ω, m, and width L.

belongs to the essential spectrum $\sigma_{\rm ess}(H)$ and the corresponding states Ψ_a represent BICs.

We illustrate two configurations of the electrostatic dots in the nanoribbon in Fig. 1 where the bound-state energy $E = m$ will be a discrete energy in the gap or will be embedded into the continuum spectrum in the second case, for $j = 0$ and $j = 1$, respectively.

B. Quantum dots in metallic AGNR

Let us consider now the setting where we fix $M_2 = M_1$, i.e., $\alpha = 0$. In this case, there is no gap in the essential spectrum Eq. (18) and the nanoribbon is metallic. We alter the electrostatic field Eqs. (20) to match its period with the width of the nanoribbon in the following manner:

$$T = \frac{L}{j}, \quad j = 1, 2, 3, \ldots. \tag{33}$$

We can achieve it by fixing $m \equiv m_j$ and $\omega \equiv \omega_j$ such that

$$m_j^2 + \omega_j^2 = \frac{\pi^2 j^2}{L^2}, \quad j = 1, 2, 3, \ldots. \tag{34}$$

In the construction of bound states confined by these quantum dots, we can follow exactly the same steps as in the previous subsection. We define

$$\Psi_a = (\mathbf{1} + P_0 M_1) v_a(x, y), \quad H\Psi_a = m_j \Psi_a, \quad a = 1, 2, 3, 4. \tag{35}$$

Due to Eq. (33), the bispinors Eqs. (25) are $2L$ periodic, and there holds, in particular,

$$v_a(L, y) = M_1 M_2 v_a(-L, y) = v_a(-L, y). \tag{36}$$

It is possible to show that the the eigenstates Ψ_a comply with the required boundary conditions and represent Dirac fermions confined by the electrostatic field. They are BICs as their energy $E = m_j$ is embedded in the essential spectrum:

$$m_j \in \sigma_{\rm ess}(H). \tag{37}$$

We illustrate the potential together with the probability of density of states in Fig. 3.

IV. CONCLUSIONS

Our results show that the localized electric field can confine Dirac fermions with energies that are either in the gap or embedded in the continuum. In our models, the match between the period of the electric field and the width of the nanoribbons, Eq. (28) or (33), allowed us to find the localized solutions analytically at the fixed energy $E = m$. When the width of the nanoribbon is mismatched with the period

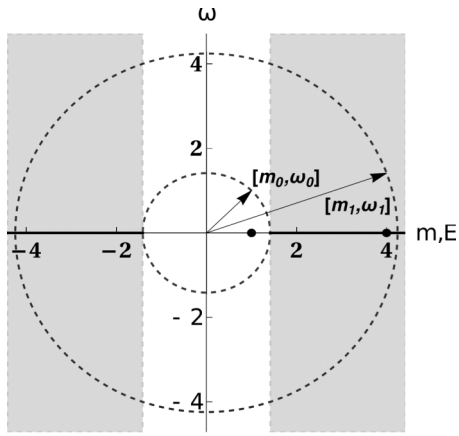

FIG. 2. The electrostatic potential Eqs. (20) is uniquely fixed by the choice of the parameters ω and m. The eligible values of the parameters have to satisfy Eqs. (28), which implies that $m_j^2+\omega_j^2=\frac{\pi^2(2j+1)^2}{4L^2}$, $j=0,1,2,....$ Note that $\omega m\neq 0$ as the electrostatic field would vanish otherwise. The two dashed circles correspond to $j=0$ and $j=1$. The parameter m_j corresponds to the bound-state energy (black dots). The horizontal axis m can be also identified with the energy axis. The shaded half planes (black semilines on m,E axis) correspond to bands of essential spectrum $\sigma_{\rm ess}(H)=(-\infty,-\frac{\pi}{2L}]\cup[\frac{\pi}{2L},\infty)$. For any $j>0$, we can select m_j such that it belongs to the essential spectrum. In the figure, $[m_0,\omega_0]$ and $[m_1,\omega_1]$ are fixed in coherence with their values used in Fig. 1. $E=m_0$ is discrete energy, $E=m_1$ corresponds to BIC.

of the potential, we expect the confined states with *discrete* energies to keep existing in the system. Nevertheless, their energy would depart from value m and their form would not be calculable analytically. The BICs are more fragile with respect to perturbations [31]. Therefore, we expect that they would turn into long-life resonance states in the case of imperfections of the electrostatic potential. Remark that analytical solutions for bound states with nonzero energy are quite unusual in the literature where mainly zero modes confined by electrostatic potentials are considered [20–22,45–47].

Our models can serve for perturbative analysis of bound states in the systems with generalized form of electrostatic dots. In this way, they can provide insight into a wider class of settings where analytical treatment is not possible. Recent advances in fine tuning of electrostatic quantum dots [28] suggest that the settings similar to those discussed in the current paper could be reachable experimentally in the near future.

The BICs are rather difficult to observe in the experiments directly as they do not couple to the propagating modes and, therefore, they do not contribute to the electronic transport. Nevertheless, it seems to be possible to prove their existence by simultaneous measurements of local density of states (LDOS) and conductance. There were theoretical studies on the existence of BICs in graphene nanoribbons. In Ref. [32], the BICs were found in the nanoribbon with variable width. In Ref. [33], BICs were observed by in the system where trilayer graphene flakes in an AAA configuration was connected to armchair nanoribbon leads. In both cases, the tight-binding calculations showed that BIC has no influence on the transport properties. Yet, they correspond to delta function peaks in LDOS. When a perturbation is introduced, e.g., by applying voltage on the trilayer graphene flake, BICs get coupled to the propagating modes and contribute to the conductance. Therefore, the combination of LDOS and conductance calculations can prove the existence of BICs in these systems. The BICs can also play an essential role in the control of absorption of light by graphene with the use of dielectric metasurfaces, see, e.g., Refs. [34,35] where ultrasensitive absorption characteristics for graphene-based devices were achieved.

The electrostatic field Eqs. (20) lacks both translational and rotational symmetry. To our best knowledge, such configuration of the electric field in graphene nanoribbons have not been discussed in the literature so far. We believe that the presented results improve our understanding of electronic properties of Dirac fermions in graphene and arm-chair nanoribbons in particular. We also think that our analysis, based on reflection and periodic symmetries, can inspire further investigation of analytically solvable models of Dirac fermions in graphene nanoribbons with electrostatic field. We plan to report on our progress along this line in the near future.

ACKNOWLEDGMENTS

V.J. was supported by Czech Science Foundation (GAČR) Grant No.19-07117S. Partial financial support is acknowledged from the Ministry of Science of Spain No. PID2020-113406GB-I0 and to Junta de Castilla y León No. BU229P18. V.J. and Ş.K. would like to thank Departamento de Física Teórica, Atómica y Óptica, Universidad de Valladolid, for warm hospitality.

APPENDIX

Let us have a system described by the Hamiltonian $H=H_0+V(x,y)$, where $V(x,y)$ can be an arbitrary Hermitian matrix with position-dependent entries. We set the following boundary condition in $x=0$ and $x=L$:

$$\Psi(0,y)=M_1\Psi(0,y),\quad \Psi(L,y)=M_2\Psi(L,y),$$
$$M_1^2=M_2^2=\mathbf{1}. \tag{A1}$$

We suppose that

$$[P_0M_1,H_0]=0,\quad [P_0M_1,V]=0, \tag{A2}$$

where P_0 is reflection at $x=0$, $P_0f(x,y)=f(-x,y)$. The first commutator in Eqs. (A2) implies that the matrix M_1 has the following form:

$$M_1=\boldsymbol{\nu}.\boldsymbol{\tau}\otimes\sigma_2, \tag{A3}$$

where the real vector $\boldsymbol{\nu}$ is arbitrary. Therefore, there holds $[P_0M_1,H_0]=0$ both for armchairlike boundaries specified by Eq. (7) and for the infinite-mass boundary conditions given by Eqs. (6) with $\nu=\pi/2$. We suppose that the potential $V(x,y)$ is such that the second commutator in Eqs. (A2) is vanishing as well. This is particularly the case for the electrostatic interaction $V(x,y)=v(x,y)\mathbf{1}$ that is even in x.

Let us take a generic solution $F=F(x,y)$ of $(H-E)F(x,y)=0$. We define the function Ψ,

$$\Psi(x,y)=(\mathbf{1}+P_0M_1)F(x,y), \tag{A4}$$

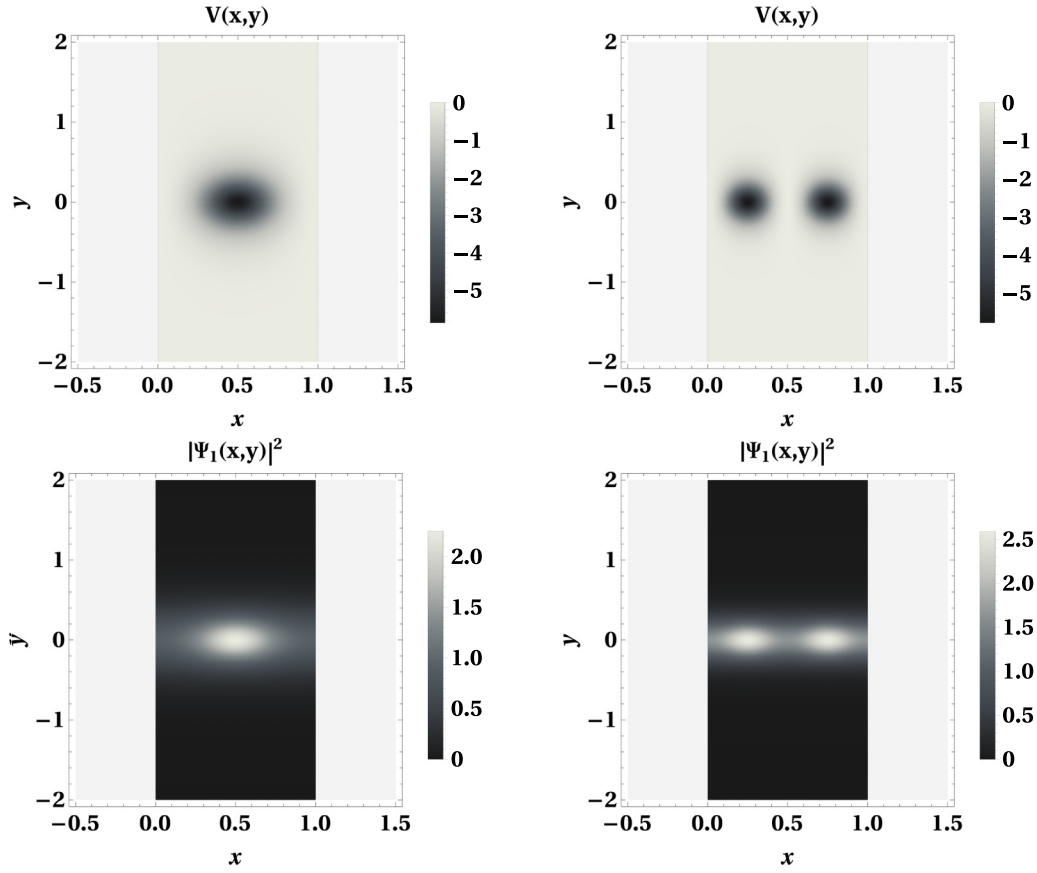

FIG. 3. Top: Density of probability of (normalized) Ψ_1 in Eqs. (35) for the boundary matrices $M_1 = M_2$. Botttom: Electrostatic potential $V(x, y)$ in Eqs. (20). We fixed $m_1 = 2$, $T_1 = L$ (left) $m_2 = 5$, $T_2 = \frac{L}{2}$ (right). $L = 1$ and $\omega_j = \sqrt{\frac{\pi^2}{T_j^2} - m_j^2}$, $j = 1, 2$ in all cases. It is worth noticing that similar electrostatic quantum dots in armchair nanoribbons created by STM tips were considered in Ref. [11].

that is, an eigenstate of H. It is straightforward to see that the function Ψ satisfies the boundary conditions in $x = 0$ by construction, $\Psi(0, y) = M_1\Psi(0, y)$. The formula Eq. (A4) represents a simple way how to construct spinors that follow the boundary condition at $x = 0$ from a generic solution $F(x, y)$ of the stationary equation $(H - E)F(x, y) = 0$.

We require Ψ to satisfy the boundary conditions at $x = L$. Substituting Eq. (A4) into the second relation in Eqs. (A1), the corresponding equation can be brought into the following form:

$$(\mathbf{1} - M_2)(F(L, y) - M_2M_1F(-L, y)) = 0. \tag{A5}$$

Therefore, when $F(x, y)$ satisfies

$$F(L, y) = M_2M_1F(-L, y), \tag{A6}$$

the wave function Ψ in Eq. (A4) satisfies the required boundary conditions Eqs. (A1).

[1] M. I. Katsnelson, K. S. Novoselov, and A. K. Geim, Chiral tunneling and the Klein paradox in graphene, Nat. Phys. **2**, 620 (2006).

[2] H.-Y. Chen, V. Apalkov, and T. Chakraborty, Fock-Darwin States of Dirac Electrons in Graphene-Based Artificial Atoms, Phys. Rev. Lett. **98**, 186803 (2007).

[3] A. Matulis and F. M. Peeters, Quasibound states of quantum dots in single and bilayer graphene, Phys. Rev. B **77**, 115423 (2008).

[4] P. Hewageegana and V. Apalkov, Electron localization in graphene quantum dots, Phys. Rev. B **77**, 245426 (2008).

[5] J. H. Bardarson, M. Titov, and P. W. Brouwer, Electrostatic Confinement of Electrons in an Integrable Graphene Quantum Dot, Phys. Rev. Lett. **102**, 226803 (2009).

[6] J.-S. Wu and M. M. Fogler, Scattering of two-dimensional massless Dirac electrons by a circular potential barrier, Phys. Rev. B **90**, 235402 (2014).

[7] T D Linh Dinh, H. Chau Nguyen, and V. Lien Nguyen, Quasi-bound states in single-layer graphene quantum rings, J. Phys.: Condens. Matter **30**, 315501 (2018).

[8] H. Chau Nguyen, M. Tien Hoang, and V. Lien Nguyen, Quasi-bound states induced by one-dimensional potentials in graphene, Phys. Rev. B **79**, 035411 (2009).

[9] P. Silvestrov and K. Efetov, Quantum Dots in Graphene, Phys. Rev. Lett. **98**, 016802 (2007).

[10] B. Zhou, B. Zhou, W. Liao, and G. Zhou, Electronic transport for armchair graphene nanoribbons with a potential barrier, Phys. Lett. A **374**, 761 (2010).

[11] D. Żebrowski, A. Mreńca-Kolasińska, and B. Szafran, Aharonov-Bohm conductance oscillations and current equilibration in local n-p junctions in graphene, Phys. Rev. B **98**, 155420 (2018).

[12] B. Trauzettel, D. V. Bulaev, D. Loss, and G. Burkard, Spin qubits in graphene quantum dots, Nat. Phys. **3**, 192 (2007).

[13] S.-Y. Li and L. He, Recent progresses of quantum confinement in graphene quantum dots, Front. Phys. **17**, 33201 (2022).

[14] Y. Zhao, J. Wyrick, F. D. Natterer, J. Rodriguez-Nieva, C. Lewandowski, K. Watanabe, T. Taniguchi, L. Levitov, N. B. Zhitenev, J. A. Stroscio *et al.*, Creating and probing electron whispering-gallery modes in graphene, Science **348**, 672 (2015).

[15] R. R. Hartmann, N. J. Robinson, and M. E. Portnoi, Smooth electron waveguides in graphene, Phys. Rev. B **81**, 245431 (2010).

[16] D. A. Stone and C. A. Downing, and M. E. Portnoi, Searching for confined modes in graphene channels: The variable phase method, Phys. Rev. B **86**, 075464 (2012).

[17] R. R. Hartmann and M. E. Portnoi, Two-dimensional Dirac particles in a Pöschl-Teller waveguide, Sci. Rep. **7**, 11599 (2017).

[18] A. Schulze-Halberg and A. M. Ishkhanyan, Darboux partners of Heun-class potentials for the two-dimensional massless Dirac equation, Ann. Phys. **421**, 168273 (2020).

[19] Y. Avishai and Y. B. Band, Klein bound states in single-layer graphene, Phys. Rev. B **102**, 085435 (2020).

[20] C. A. Downing, D. A. Stone, and M. E. Portnoi, Zero-energy states in graphene quantum dots and rings, Phys. Rev. B **84**, 155437 (2011).

[21] C. A. Downing, A. R. Pearce, R. J. Churchill, and M. E. Portnoi, Optimal traps in graphene, Phys. Rev. B **92**, 165401 (2015).

[22] S. Kuru, J. Negro, L. M. Nieto, and L. Sourrouille, Massive and massless two-dimensional Dirac particles in electric quantum dots, arXiv:2104.06676.

[23] A. C. S. Nascimento, R. P. A. Lima, M. L. Lyra, and J. R. F. Lima, Electronic transport on graphene armchair-edge nanoribbons with Fermi velocity and potential barriers, Phys. Lett. A **383**, 2416 (2019).

[24] A. Contreras-Astorga, F. Correa, and V. Jakubský, Super-Klein tunneling of Dirac fermions through electrostatic gratings in graphene, Phys. Rev. B **102**, 115429 (2020).

[25] J. Lee, D. Wong, J. Velasco, J. F. Rodriguez-Nieva, S. Kahn, H.-Z. Tsai, T. Taniguchi, K. Watanabe, A. Zettl, F. Wang, L. S. Levitov, and M. F. Crommie, Imaging electrostatically confined Dirac fermions in graphene quantum dots, Nat. Phys. **12**, 1032 (2016).

[26] Ch. Gutiérrez, L. Brown, Ch.-J. Kim, J. Park, and A. N. Pasupathy, Klein tunnelling and electron trapping in nanometre-scale graphene quantum dots, Nat. Phys. **12**, 1069 (2016).

[27] K.-K. Bai, J.-B. Qiao, H. Jiang, H. Liu, and L. He, Massless Dirac fermions trapping in a quasi-one-dimensional n p n junction of a continuous graphene monolayer, Phys. Rev. B **95**, 201406(R) (2017).

[28] Y. Jiang, J. Mao, D. Moldovan, M. R. Masir, G. Li, K. Watanabe, T. Taniguchi, F. M. Peeters, and E. Y. Andrei, Tuning a circular p-n junction in graphene from quantum confinement to optical guiding, Nat. Nanotechnol. **12**, 1045 (2017).

[29] J.-B. Qiao, H. Jiang, H. Liu, H. Yang, N. Yang, K.-Y. Qiao, and L. He, Bound states in nanoscale graphene quantum dots in a continuous graphene sheet, Phys. Rev. B **95**, 081409(R) (2017).

[30] J. von Neumann and E. Wigner, Über merkwürdige diskrete Eigenwerte, Phys. Z. **30**, 465 (1929).

[31] Ch. W. Hsu, B. Zhen, A. D. Stone, J. D. Joannopoulos, and M. Soljačić, Bound states in the continuum, Nat. Rev. Mater. **1**, 16048 (2016).

[32] J. W. González, M. Pacheco, L. Rosales, and P. A. Orellana, Bound states in the continuum in graphene quantum dot structures, Europhys. Lett. **91**, 66001 (2010).

[33] N. Cortés, L. Chico, M. Pacheco, L. Rosales, and P. A. Orellana, Bound states in the continuum: Localization of Dirac-like fermions, Europhys. Lett. **108**, 46008 (2014).

[34] M. Zhang and X. Zhang, Ultrasensitive optical absorption in graphene based on bound states in the continuum, Sci. Rep. **5**, 8266 (2015).

[35] X. Wang, J. Duan, W. Chen, Ch. Zhou, T. Liu, and S. Xiao, Controlling light absorption of graphene at critical coupling through magnetic dipole quasi-bound states in the continuum resonance, Phys. Rev. B **102**, 155432 (2020).

[36] A. R. Akhmerov and C. W. J. Beenakker, Boundary conditions for Dirac fermions on a terminated honeycomb lattice, Phys. Rev. B **77**, 085423 (2008)

[37] L. Brey and H. A. Fertig, Electronic states of graphene nanoribbons studied with the Dirac equation, Phys. Rev. B **73**, 235411 (2006).

[38] P. Freitas and P. Siegl, Spectra of graphene nanoribbons with armchair and zigzag boundary conditions, Rev. Math. Phys. **26**, 1450018 (2014).

[39] E. McCann and V. I. Fal'ko, Symmetry of boundary conditions of the Dirac equation for electrons in carbon nanotubes, J. Phys.: Condens. Matter **16**, 2371 (2004).

[40] H. Huang, D. Wei, J. Sun, S. L. Wong, Y. P. Feng, A. H. Castro Neto, and A. T. S. Wee, Spatially resolved electronic structures of atomically precise armchair graphene nanoribbons, Sci. Rep. **2**, 983 (2012).

[41] A. H. Castro Neto, F. Guinea, N. M. R. Peres, K. S. Novoselov, and A. K. Geim, The electronic properties of graphene, Rev. Mod. Phys. **81**, 109 (2009).

[42] J. A. M. van Ostaay, A. R. Akhmerov, C. W. J. Beenakker, and M. Wimmer, Dirac boundary condition at the reconstructed zigzag edge of graphene, Phys. Rev. B **84**, 195434 (2011).

[43] J.-C. Cuenin and P. Siegl, Eigenvalues of one-dimensional non-self-adjoint Dirac operators and applications, Lett. Math. Phys. **108**, 1757 (2018).

[44] C. Gutierrez, D. Walkup, F. Ghahari, C. Lewandowski, J. F. Rodriguez-Nieva, K. Watanabe T. Taniguchi, L. S. Levitov, N. B. Zhitenev, J. A. Stroscio *et al.*, Interaction-driven quantum Hall wedding cake-like structures in graphene quantum dots, Science **361**, 789 (2018).

[45] C.-L. Ho and P. Roy, On zero energy states in graphene, Europhys. Lett. **108**, 20004 (2014).

[46] A. Schulze-Halberg and P. Roy, Construction of zero-energy states in graphene through the supersymmetry formalism, J. Phys. A: Math. Theor. **50**, 365205 (2017).

[47] C. A. Downing and M. E. Portnoi, Zero-energy vortices in Dirac materials, Phys. Status Solidi B **256**, 1800584 (2019).